

## 1            **Structural integrity monitoring of onshore wind turbine concrete foundations**

2            Magnus Currie<sup>1\*</sup>, Mohamed Saafi<sup>2\*</sup>, Christos Tachtatzis<sup>3</sup> and Francis Quail<sup>4</sup>

3            <sup>1</sup>E D P Renewables Ltd, Edinburgh, EH2 2BY, UK

4            <sup>2</sup>Department of Engineering, Lancaster University, Lancaster, LA1 4YR, UK

5            <sup>3</sup>School of Engineering, University of Glasgow, Glasgow, G12 8QQ, UK

6            <sup>4</sup>Aramco Technology Office, Aberdeen, AB32 6FE

### 7            **Abstract**

8            Signs of damage around the bottom flange of the embedded ring were identified in a large  
9            number of existing onshore concrete foundations. As a result, the embedded ring experienced  
10           excessive vertical displacement. A wireless structural integrity monitoring (SIM) technique was  
11           developed and installed in the field to monitor the stability of these turbines by measuring the  
12           displacement patterns and subsequently alerting any significant movements of the embedded  
13           ring. This was achieved by using wireless displacement sensors located in the bottom of the  
14           turbine. A wind turbine was used as a test bed to evaluate the performance of the SIM system  
15           under field operating conditions. The results obtained from the sensors and supervisory control  
16           and data acquisition (SCADA) showed that the embedded ring exhibited significant vertical  
17           movement especially during periods of turbulent wind speed and during shut down and start up  
18           events. The measured displacement was variable around the circumference of the foundation as  
19           a result of the wind direction and the rotor uplift forces. The excessive vertical movement was  
20           observed in the side where the rotor is rotating upwards. The field test demonstrated that the  
21           SIM technique offers great potential for improving the reliability and safety of wind turbine  
22           foundations.

23

24 Keywords

25 Onshore wind turbine, Concrete foundations, Forensic investigation, Structural integrity,  
26 Monitoring.

27 \*Corresponding authors ([magnus.currie@gmail.com](mailto:magnus.currie@gmail.com)) and [m.saafi@lanacaster.ac.uk](mailto:m.saafi@lanacaster.ac.uk)

28

29

## 30 **1. Introduction**

31 Wind is currently considered as one of the most cost-effective large-scale alternative energy  
32 sources. In the UK, onshore wind farm developments make up the largest proportion of wind  
33 generating capacity, with offshore production beginning to significantly grow. Structural  
34 integrity monitoring (SIM) has become an integral part of onshore wind farm asset management  
35 programs to ensure safety and reliability. Like any other structure, a wind turbine is prone to  
36 damage from fatigue, environmental exposures and construction defects. Structural problems  
37 that can affect the operation of a wind turbine could include delamination of the blade and failure  
38 of tower and foundation systems. The foundation failure is often a slow process, developing  
39 over a number of months or even years. However, recently, excessive vertical movement has  
40 been reported in several onshore wind turbine concrete foundations with embedded ring as a  
41 connection system [1]. These embedded rings have been recorded to be moving up to 20 mm or  
42 more in some extreme cases and this could lead to catastrophic collapse of the turbines. Whilst  
43 there is no published data on the exact number of failures due to commercial reasons, it is  
44 thought that the problem is widespread given the popularity of the foundation system worldwide.

45 There are 4000 wind turbines of the type operational worldwide with further manufacturers also  
46 using the foundation type.

47 SIM systems are widely used in various components, structures and sub systems of a wind  
48 turbine to allow proactive maintenance and ensure reliability and availability of the machine [2].  
49 For example, SIM systems have been applied to wind turbines to monitor blade delamination  
50 using fibre optic sensors [3] and blade icing using thermal and acoustic sensors [4]. Wireless  
51 monitoring technologies have also been suggested in order to limit the extra weight added to the  
52 blade [5]. The turbine tower generally has an extremely low failure rate [6] and hence there has  
53 been limited SIM applications. One study used strain gauge arrays to monitor the tower at a  
54 number of locations from the bottom to the top of the tower [7]. The array layout meant changes  
55 in tower modes due to wind direction could be monitored. In addition to new sensor  
56 technologies, the application of wireless communication has made SIM more practical and  
57 affordable. Research has been undertaken to assess the opportunities to apply wireless SIM to  
58 many wind turbine parts including the rotor and tower [8].

59 There are a number of different foundations types used globally, and as foundations sizes  
60 increase as turbines become larger, it becomes more important that foundations are designed and  
61 monitored effectively, both during construction and throughout their operational lifetime [9].  
62 However, currently there are no real time SIM systems in place for the operator to assist in its  
63 monitoring of the problem, mapping or quantifying the movement patterns of the foundation and  
64 subsequently alerting any potential failure.

65 In this paper, we present a wireless SIM system for onshore wind turbine concrete  
66 foundations. First, a site investigation was conducted i) to identify the main damage  
67 mechanisms responsible for the excessive vertical movement of the embedded ring, ii) to

68 determine the monitoring system requirements and iii) to develop movement alarm bands.  
69 Then, a wireless sensor array system was designed and deployed in one wind turbine foundation  
70 to monitor its vertical movement under normal turbine operating conditions. The reliability of  
71 the monitoring system and the response of the individual sensors were assessed and compared to  
72 SCADA data. The structural response of the concrete foundation was quantified under turbine  
73 operational conditions and the effect of wind speed and direction on the vertical movement of the  
74 foundation was analysed.

## 75 **2. Wind turbine test bed**

76 The onshore wind turbine concrete foundations with embedded ring shown in Fig. 1 are widely  
77 used around the world. These types of foundations are the subject of this study with respect to  
78 vertical movement. Several wind farms were visited to identify the main cause of this vertical  
79 movement using Endoscopic filming through boreholes created in the foundations. The  
80 Endoscopic filming showed significant voids filled with water under the flange of the embedded  
81 ring. Significant erosion was also observed on the upper side of bottom flange due to the uplift  
82 forces placed on the foundation by the rotor. These voids have caused excessive vertical  
83 movement of the ring, leading to concrete cracking (Fig. 2) and failure of the water proofing  
84 system.

85 Based on the site observations, the followings vertical movement bandings were used as  
86 warning signals. Normal operation allows 1-2 mm of elastic stretching of the tower, 3-4 mm of  
87 vertical movement is a sign that there is voids in the foundation and finally movement over 5  
88 mm is deemed to be serious and further investigations are necessary. When the SIM records a  
89 movement of 5 mm or greater, the foundation requires remediation. Accordingly, a sensor  
90 sensitivity of 0.1 mm was adopted for the SIM system.

91 The wind turbine test bed used in this investigation was a modern 2.0 MW pitch regulated  
92 variable speed machine and in operation for at least five years. The exact location and turbine  
93 model are confidential due to a non-disclosure agreement with the operator. The foundation  
94 consisted of an octagonal reinforced concrete slab with an embedded steel ring connection  
95 system. Fig. 3 shows the geometry of the foundation. The foundation was designed to support a  
96 67 m-hub tower equipped with a rotor of 80 m in diameter.

### 97 **3. Wireless SIM methodology**

98 Currently, monitoring of vertical movement involves visits by technicians to the site to take  
99 manual readings of the foundation movement. This can be problematic during winter when the  
100 site is often partially or fully inaccessible due to snow cover and/or high winds. Furthermore,  
101 the greatest displacement occurs during higher wind speeds and this cannot be guaranteed during  
102 each visit. Consequently, a SIM solution needed to allow more accurate and detailed real time  
103 movement data. The SIM system presented in this paper was designed to provide a much greater  
104 level of data to the engineering team than was previously available using site investigation  
105 techniques alone.

106 In this project, linear variable differential transformer (LVDT) sensors were adopted to  
107 measure the vertical movement of the embedded ring. LVDTs sensors are a very effective  
108 method for measuring movement and have been used in a number of SIM applications in civil  
109 engineering structures [10]. They are robust and immune to large magnetic field surrounding the  
110 high voltage cables coiled in the foundation. LVDTs with a gauge length of 50 mm were  
111 selected as being the optimum size and having a suitable accuracy for the displacement  
112 measurements.

113 As shown in Fig. 4a, four LVDT sensors were installed under the top flange of the embedded  
114 ring. Each LVDT was equipped with an off-the-shelf wireless communication node set to  
115 measure displacement at a frequency of 1Hz. This rate was deemed to be sufficient for the  
116 relatively slow movement of the turbine tower. The nodes were equipped with a 2.4 GHz  
117 CC2420 wireless radio chip from Texas Instruments, which is IEEE 802.15.4 compliant. The  
118 transmission power was set at 0 dBm while the receiver sensitivity of radio chip is -95 dBm.  
119 The wireless gateway device consisted of an off-the-shelf low cost Raspberry Pi microcomputer,  
120 a standard 4GB SD memory card and a small size battery pack, which acts as a UPS.

121 The sensors were positioned equidistant around the foundation (see Fig. 4a). The measurement  
122 points are numbered on the figure as 1 NW (North West), 2 NE (North East), 3 SE (South West)  
123 and 4 SW (South West). These points were selected because the prevailing wind conditions on  
124 the site were south-westerly in nature. Using these measurement points, the sensor array would  
125 capture the displacement on planes parallel and perpendicular to the prevailing wind. The LVDT  
126 sensors were installed to measure the displacement between the static concrete foundation and  
127 the embedded ring. It was essentially measuring the movement of the embedded ring at the  
128 connection with the tower. Retort stands were used to keep the sensors with a heavy weight base  
129 and the attachments were locked in position using thumbscrews, preventing any movement  
130 during operation. The LVDTs were set half compressed, allowing vertical upwards and  
131 downwards movements to be recorded. The LVDT installed in the foundation had a maximum  
132 stroke of 50 mm; hence they were installed at a set position of 25 mm. Fig. 4-b shows the sensor  
133 location along with the method of anchoring the sensor.

134 The monitoring of the foundation was carried out over a period of 2 months to evaluate the  
135 performance of the SIM system under field conditions using a remote data acquisition system.

136 SCADA data was collected and correlated with the measured displacements. The data included  
137 wind speed, wind direction and rotational speed of the rotor. Maximum and minimum wind  
138 speed and standard deviations were obtained for each variable and used to evaluate the response  
139 of the foundation under the turbine operating conditions. The recorded displacements were  
140 compared with the maximum rotational speed since this was the key-influencing factor on the  
141 displacement of the foundation

#### 142 **4. Results and discussion**

##### 143 *4.1. Effect of rotor and wind speed on the vertical displacement of the embedded ring*

144 Fig. 5a depicts the structural response of the embedded ring subjected to dynamic loading during  
145 the turbine operating conditions over a period of 30 min. As can be seen, large drop offs in the  
146 maximum rotor speed were observed. This was due to the drop in the wind speed. The standard  
147 deviation of mean rotor speed exhibited peaks higher than 0.6, suggesting a period of turbulence.  
148 The spikes in the ring displacement occurred in line with the standard deviation peak. This  
149 means that during periods of turbulent wind, the rotor is subjected to sudden acceleration and  
150 deceleration. This sudden change in the momentum resulted in the ring lifting and falling of the  
151 embedded ring. This suggests that the embedded ring experiences vertical displacement during  
152 sudden acceleration and deceleration of the rotor resulting from the change in the wind speed and  
153 direction. Vertical displacement could also occur during shut down and start up events as this  
154 produces sudden acceleration and deceleration of the rotor. Figure 5b shows a number of peak  
155 displacements up to 5 mm. In this case, some of the peaks appeared to be related to the rotor  
156 speed standard deviation e.g. turbulence, whilst others, such as at 19:12, appeared to be related to  
157 the maximum rotor speed peaks.

158 As shown in Fig. 6, the embedded ring experienced significant vertical displacement at  
159 high wind speeds. Serious displacement was deemed by the operator to be any movement over 5  
160 mm in magnitude. Most of the vertical displacement was witnessed in the rising direction with  
161 the tower settling back downwards after rotor speeds stabilised. A significant period of  
162 displacement over approximately 5 min was observed between 18:00 and 18:05. The amber and  
163 red warning lines at 3 mm and 5 mm respectively indicate the warning bands required by the  
164 operator for analysis. At 18:01 there was a large drop off in the rotor speed, which triggered  
165 large upward then large downward displacements of over 5 mm, breaching the red warning line.  
166 Five small displacement peaks between 0.5 mm and 1.5 mm were also observed. Each of these  
167 peaks correlated with the rotor speed standard deviation peaks as shown in Fig. 6.

168 High wind speeds also resulted in significant vertical displacement of the ring as indicated in  
169 Fig. 7. This illustrates one of the many variable periods of displacement observed during the  
170 monitoring period. As can be seen, rising and falling of the ring around 7 mm through 6  
171 prescribed cycles were observed over a period of 15 min. The overall displacement pattern  
172 correlated roughly with the maximum rotor speed peaks and troughs as well as with the mean  
173 rotor speed standard deviation peaks. It is clear that there was a significant ring movement  
174 tracking the significant fluctuation in the rotor speed, particularly between 19:18 and 19:25, with  
175 a full cycle occurred approximately every minute. This cyclic (rise and fall) movement would be  
176 evident to an observer on site. The displacement during this period travelled through all three  
177 warning bands, resulting in red warning alerts, which would result in a warning alarm.

## 178 5.2. *Effect of wind direction on the vertical displacement of the embedded ring*

179 Figure 8a shows the effect of the wind direction on the vertical displacement of the embedded  
180 ring. As shown, the southwesterly wind was turbulent causing rotor speed changes between 14.5



181 rpm and 16.5 rpm. As previously discussed, the displacement peaks correlated approximately  
182 with periods of the high mean rotor speed standard deviation. The NW and SW sensors picked  
183 up exactly the same movements. However, the sensor NW, orthogonal to the wind direction,  
184 recorded larger displacements at every peak. This was the result of the wind direction and  
185 ultimately the position of the rotor. It is likely that the side where the wind hit will be pushed up  
186 a little but the greatest vertical movement was observed in the side where the rotor is rotating  
187 upwards as a result of the uplift force experienced on the NW side of the foundation.

188 Figure 8b shows the displacement recorded by the NW, SW and SE sensors during a major  
189 dip in the rotor speed. The NE sensor provided a corrupted signal. It appeared that the  
190 displacement was variable around the circumference of the ring as a result of the wind direction  
191 and the rotor uplift forces. The NW side of the ring exhibited higher displacement as compared  
192 to SW and SE sides. The response of the sensor in the SE corner was slightly below zero much  
193 of the time suggesting that the foundation has eroded allowing a negative displacement below the  
194 level the sensors were set at.

## 195 **Conclusions**

196 The potential of using a low cost displacement sensor array to measure vertical movement of  
197 onshore wind turbine foundations with embedded ring is presented in this paper. The system is  
198 simple and relatively easy to install. The ability of the system to capture displacement,  
199 regardless of wind direction demonstrates the potential for further development into a full SIM  
200 system complete with user interface and alerting toolset. The site investigation identified  
201 several damage mechanisms responsible for the excessive movement of the embedded steel ring.  
202 Structural cracks were commonly observed in the concrete pedestals. Water ingress through  
203 these cracks led to the formation of voids above and underneath the bottom flange of the

204 embedded ring. The cyclic movement of the embedded ring led the erosion of the concrete and  
205 ultimately created these voids. The observed defects could have negative impact on the  
206 structural integrity of onshore wind turbines and as a result, the development of renewable  
207 energy could be hindered. Monitoring the progress of these defects is deemed necessary to  
208 prevent catastrophic failures.

209 Based on the results from the field test, the wireless SIM system picked up a number of  
210 varying movements including single and cyclic patterns. The Results also showed that the  
211 embedded ring experienced vertical movement on a number of occasions (red warning 5mm or  
212 greater movement). The excessive displacements were observed during periods of turbulent  
213 wind speeds and during shut down and start up events. The wireless system presented herein  
214 limited the number of cables in the turbine and allowed data download without need to access the  
215 turbine. The system is flexible and could handle additional sensors, different sensors types and  
216 also variable frequency of readings. The SIM system has the potential to greatly impact the  
217 onshore wind energy industry by significantly reducing both the risk of catastrophic failure of the  
218 foundations and the energy supply disruptions.

219

## 220 **Acknowledgements**

221 This work has been funded by the EPSRC, project reference number EP/G037728/1.

## 222 **References**

- 223 1. Currie M, Quail F, Saafi M. Development of a robust structural health monitoring system  
224 for wind turbine foundations. in *ASME Turbo Expo 2012*. 2012. Copenhagen: ASME.  
225
- 226 2. Schubel PJ, Crossley RJ, Boateng EKG, Hutchinson JR. Review of structural health and  
227 cure monitoring techniques for large wind turbine blades. *Renewable Energy* 2013; 51:113-123.  
228  
229
- 230 3. Bang HJ, HK Shin, YC Ju. Structural health monitoring of a composite wind turbine  
231 blade using fiber Bragg grating sensors, in *Sensors and Smart Structures Technologies for Civil,  
232 Mechanical, and Aerospace Systems 2010*; Spie-Int Soc Optical Engineering: Bellingham.

233  
234 4. Harper N. Detecting Ice on Wind-turbine Blades. Windpower Engineering 2011.  
235  
236 5. Taylor SG, Farinholt KM, Park G, Farrar CR, Todd MD. Application of a wireless sensor  
237 node to health monitoring of operational wind turbine blades 2009; Conference: 28th  
238 International Modal Analysis Conference ; February 1, 2010 ; Jacksonville, FL  
239  
240 6. Ribrant J, and Bertling LM. Survey of failures in wind power systems with focus on  
241 Swedish wind power plants during 1997-2005. Ieee Transactions on Energy Conversion 2007;  
242 22(1): 167-173.  
243  
244 7. Benedetti M, Fontanari V, Zonta D, Structural health monitoring of wind towers: remote  
245 damage detection using strain sensors. Smart Materials & Structures 2011. 20(5).  
246  
247 8. Swartz RA, Lynch JP, Zerbst S, Sweetman B, Rolfes R. Structural monitoring of wind  
248 turbines using wireless sensor networks. Smart Structures and Systems 2010; 6(3):183-196.  
249  
250 9 Wang P, Yan Y, Gui YT, Bouzid O, Ding Z. Investigation of Wireless Sensor Networks  
251 for Structural Health Monitoring. Journal of Sensors, 2012; 2012.  
252  
253 10. Ciang CC, Lee JR, Bang HJ. Structural health monitoring for a wind turbine system: a  
254 review of damage detection methods. Measurement Science & Technology 2008; 19(12).  
255 11. Texas Instruments. Single-Chip 2.4 GHz IEEE 802.15.4 Compliant and ZigBee Ready  
256 RF Transceiver (Rev. B) 2012 [cited 2013 Aug 4]; Available from:URL:  
257 <http://www.ti.com/lit/ds/symlink/cc2420.pdf>.  
258  
259 12. Di Franco F, Tachtatzis C, Graham B, Bykowski M, Tracey DC, Timmons NF, Morrison  
260 J. Current characterisation for ultra low power wireless body area networks. in Intelligent  
261 Solutions in Embedded Systems (WISES) 2010; 8th Workshop on. 2010; 91-96.  
262  
263 13. RaspberryPi. Raspberry Pi FAQs 2013 [cited 2013 17th July]; Available from: URL:  
264 <http://www.raspberrypi.org/faqs>.  
265  
266  
267  
268  
269  
270  
271  
272  
273  
274  
275  
276  
277  
278

279  
280  
281  
282  
283  
284  
285  
286  
287  
288  
289  
290  
291  
292  
293  
294  
295  
296  
297  
298  
299  
300  
301  
302  
303  
304  
305  
306  
307  
308  
309  
310  
311  
312  
313

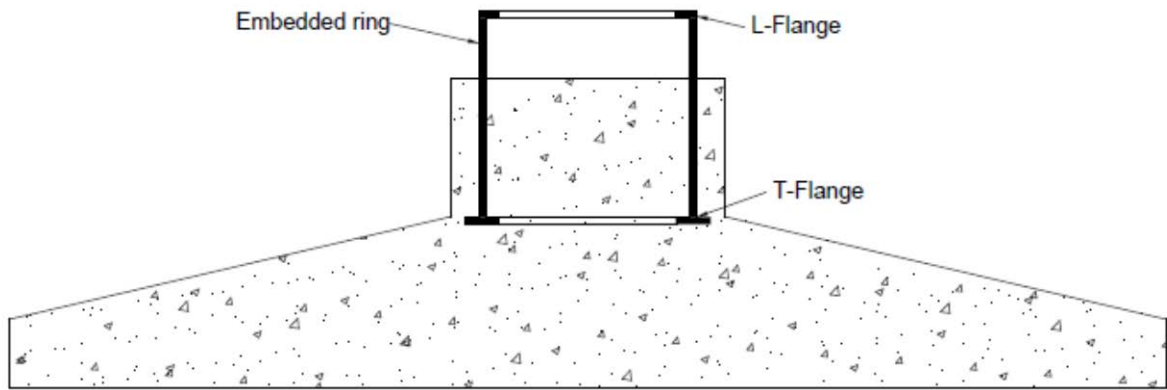


Fig.1: Typical onshore wind concrete foundation with embedded ring



314 Fig. 2 Cracked concrete foundation as a result of excessive displacement of the embedded ring.  
315

316

317

318

319

320

321

322

323

324

325

326

327

328

329

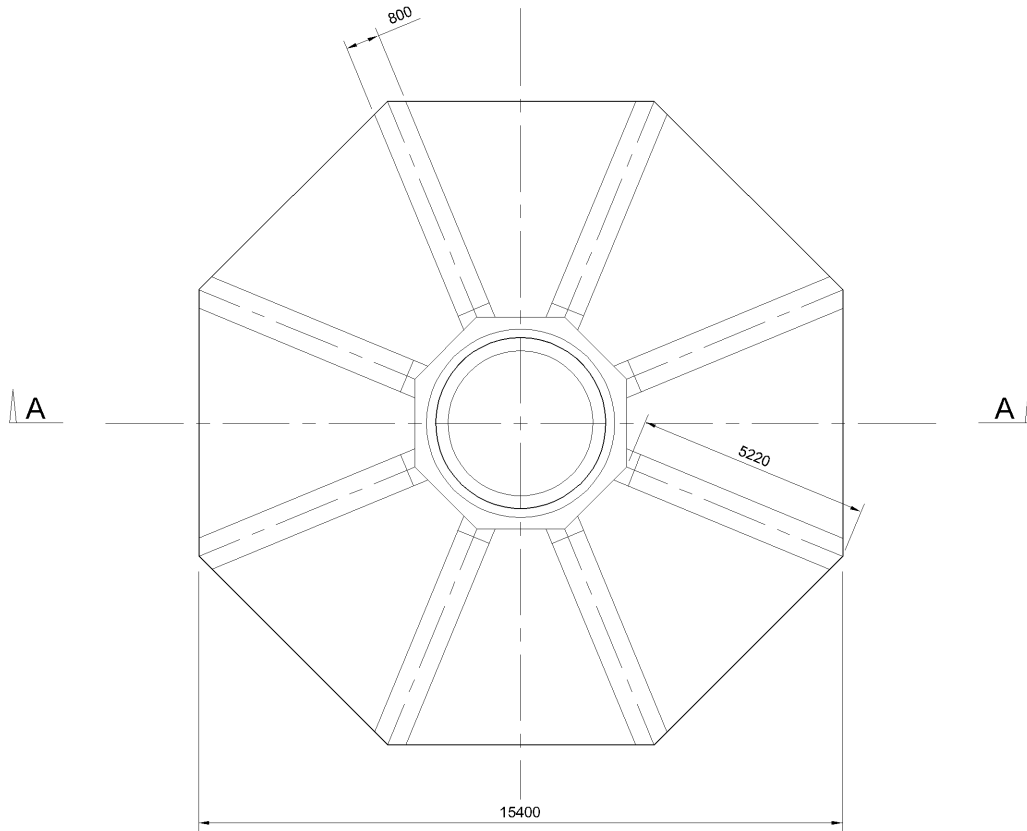
330

331

332

333

334



335 Plan

336

337

338

339

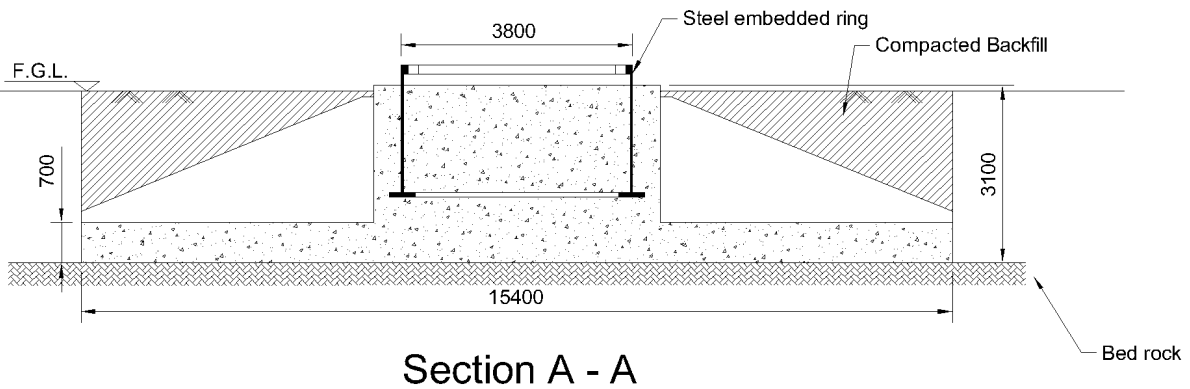
340

341

342

343

344



Section A - A

Fig. 3. Layout of the wind turbine concrete foundation (dimensions in mm)

345  
346  
347  
348  
349  
350  
351  
352  
353  
354  
355  
356  
357  
358  
359  
360  
361  
362  
363  
364  
365  
366  
367  
368  
369  
370  
371  
372  
373  
374  
375  
376  
377  
378

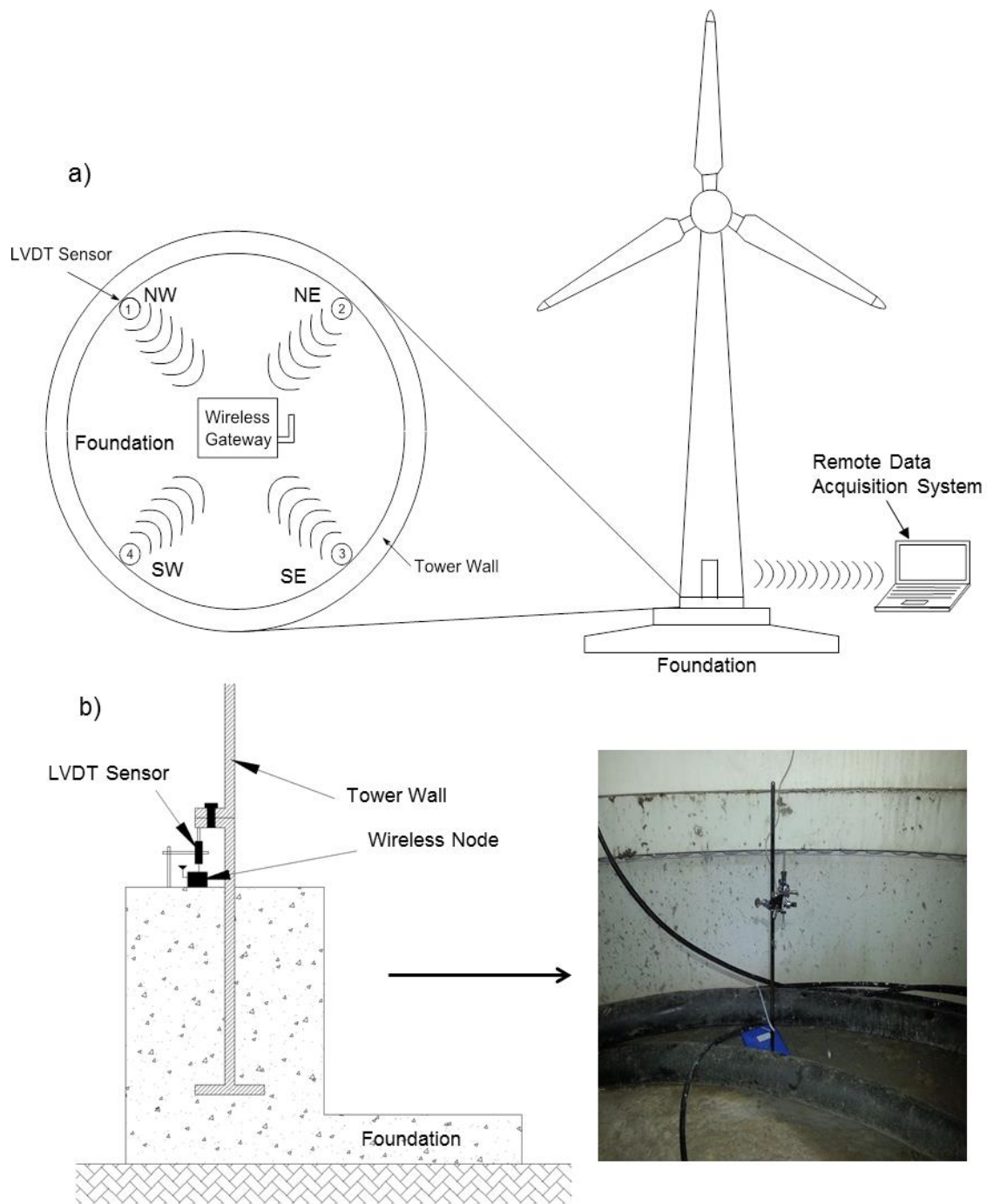
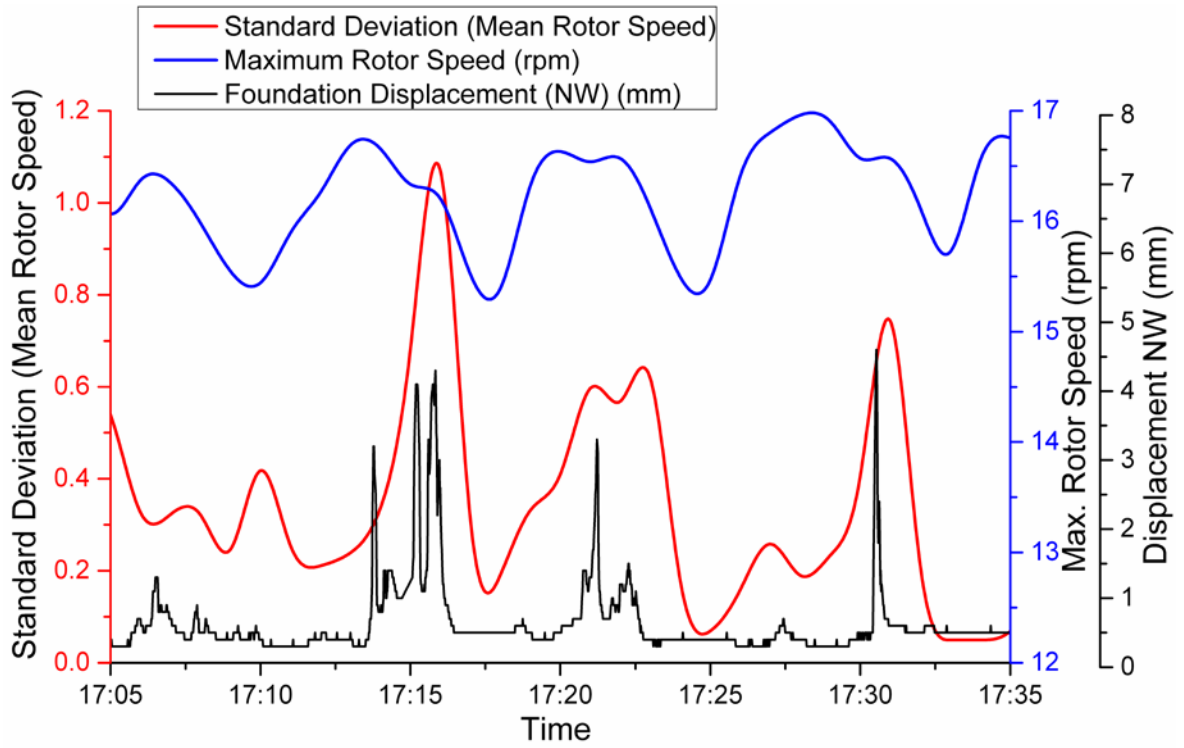


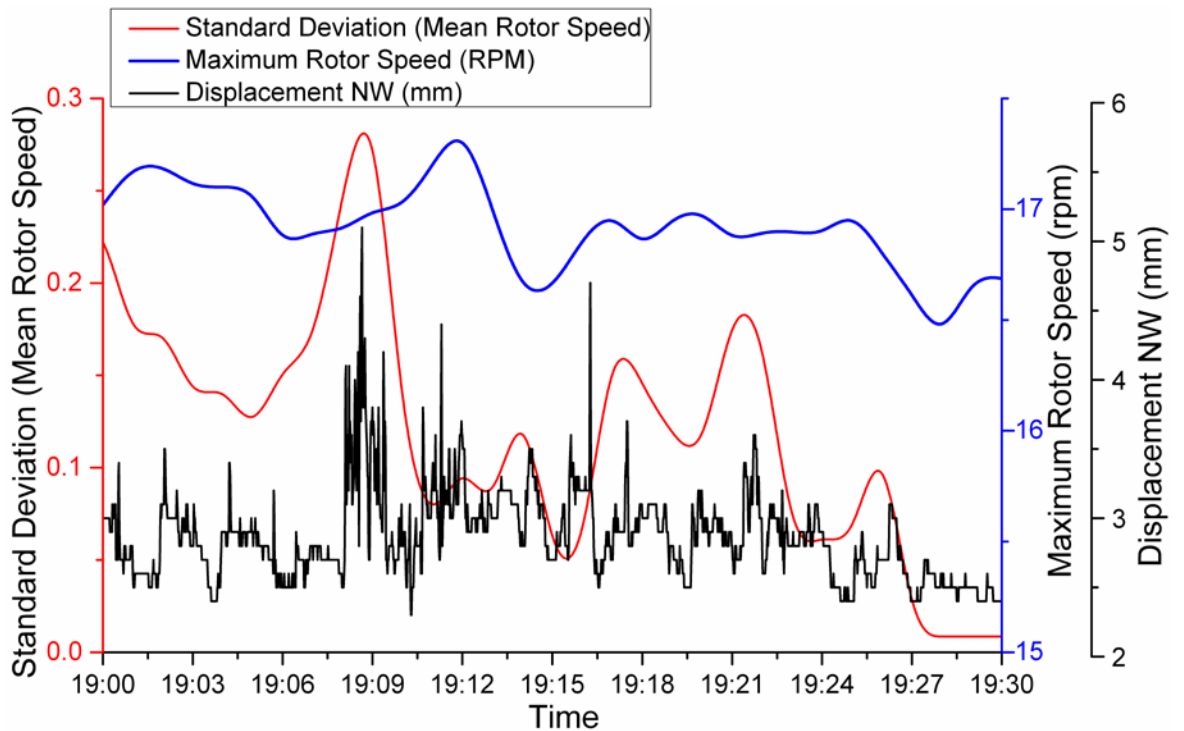
Fig. 4. a) SIM architecture and b) sensor installation.

379  
380  
381  
382  
383  
384  
385  
386  
387  
388  
389  
390  
391  
392  
393  
394  
395  
396  
397  
398  
399  
400  
401  
402  
403  
404  
405  
406  
407  
408  
409  
410

a)



b)



411

412

413 Fig. 5. Effect of rotor speed on the vertical displacement of the embedded ring.

414

415

416

417

418

419

420

421

422

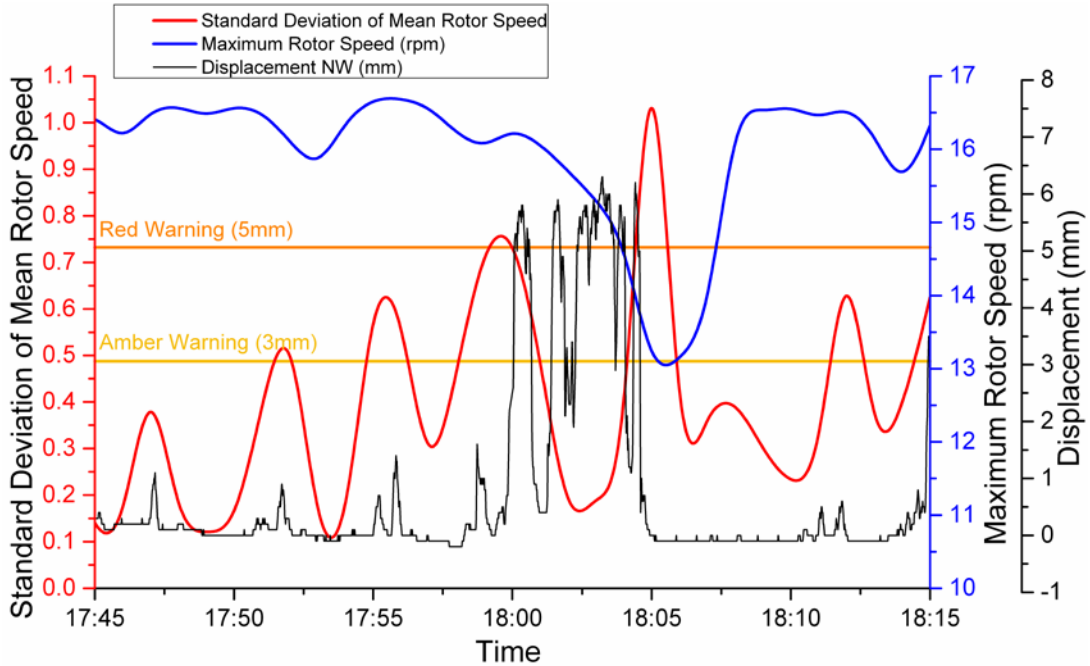
423

424

425

426

427



428 Fig. 6. Effect of high wind speed on the vertical displacement of the embedded ring.

429

430

431

432

433

434

435

436

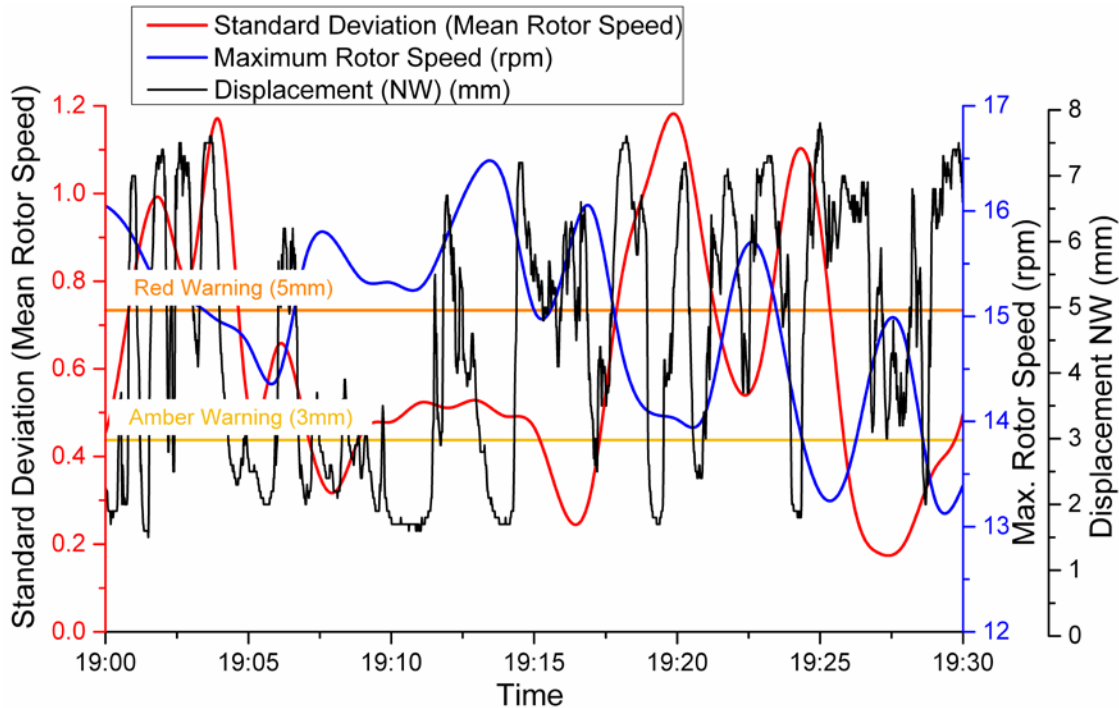
437

438

439

440

441





442

443

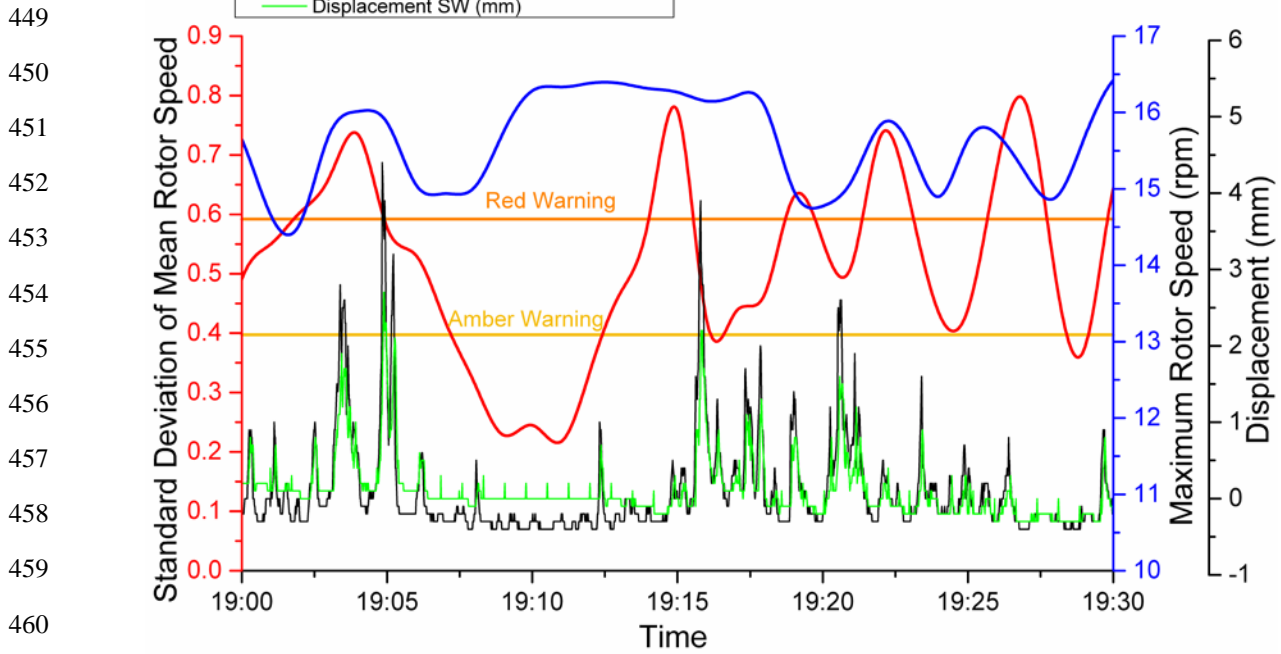
444 Fig. 7. Cyclic vertical displacement of the embedded ring as a result of high wind speed.

445

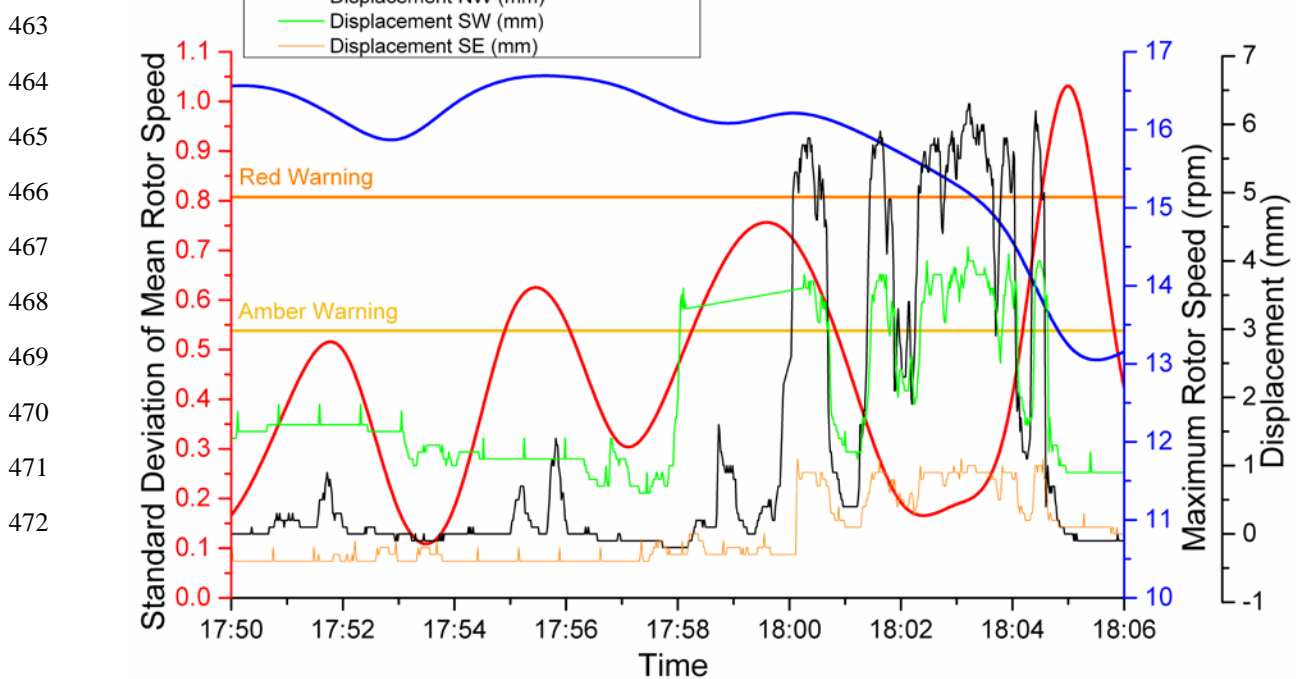
446

447

448 a)



462 b)



473

474

475 Fig. 8: Effect of wind direction on the vertical displacement of the embedded ring a) comparison  
476 between NW and SW sensors, b) comparison between NW, SW and SE sensors during a major  
477 change in the rotor speed.